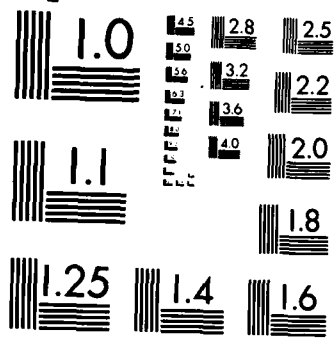END
FILMED
DTIC

MICROCOPY RESOLUTION TEST CHART

NATIONAL BUREAU OF STANDARDS-1963-A

AD-A162 114

Technical Report 1053
August 1985

COMPARISON OF THE WALL PRESSURE FLUCTUATIONS IN ARTIFICIALLY GENERATED TURBULENT SPOTS, NATURAL TRANSITION AND TURBULENT BOUNDARY LAYERS

T. S. Mautner

Naval Ocean Systems Center

San Diego, California 92152-5000

DTIC
ELECTED
DEC 1 0 1985

A

85 12 -9 064

NAVAL OCEAN SYSTEMS CENTER SAN DIEGO, CA 92152

F. M. PESTORIUS, CAPT, USN   R.M. HILLYER
Commander   Technical Director

ADMINISTRATIVE INFORMATION

JJ

AD-A162 114

REPORT DOCUMENTATION PAGE

1a. REPORT SECURITY CLASSIFICATION		1b. RESTRICTIVE MARKINGS			
UNCLASSIFIED					
2a. SECURITY CLASSIFICATION AUTHORITY		3. DISTRIBUTION/AVAILABILITY OF REPORT			
		Approved for public release; distribution unlimited.			
2b. DECLASSIFICATION/DOWNGRADING SCHEDULE					
4. PERFORMING ORGANIZATION REPORT NUMBER(S)		5. MONITORING ORGANIZATION REPORT NUMBER(S)			
NOSC TR 1053					
6a. NAME OF PERFORMING ORGANIZATION	6b. OFFICE SYMBOL (If applicable)	7a. NAME OF MONITORING ORGANIZATION			
Naval Ocean Systems Center	Code 634				
6c. ADDRESS (City, State and ZIP Code)		7b. ADDRESS (City, State and ZIP Code)			
Hydromechanics Branch San Diego, CA 92152-5000					
8a. NAME OF FUNDING/SPONSORING ORGANIZATION	8b. OFFICE SYMBOL (if applicable)	9. PROCUREMENT INSTRUMENT IDENTIFICATION NUMBER			
Naval Sea Systems Command	NSEA-63R31				
8c. ADDRESS (City, State and ZIP Code)		10. SOURCE OF FUNDING NUMBERS			
		PROGRAM ELEMENT NO.	PROJECT NO.	TASK NO	Agency Accession
Materials and Mechanics Division Washington, DC 20362-5101		61153N	SR02301	SR0230103	DN530 697

11. TITLE (include Security Classification)

COMPARISON OF THE WALL PRESSURE FLUCTUATIONS IN ARTIFICIALLY GENERATED TURBULENT SPOTS, NATURAL TRANSITION AND TURBULENT BOUNDARY LAYERS

12. PERSONAL AUTHOR(S)

T.S. Mautner

13a. TYPE OF REPORT	13b. TIME COVERED		14. DATE OF REPORT (Year, Month, Day)	15. PAGE COUNT
Final	FROM _____	TO _____	August 1985	16

16. SUPPLEMENTARY NOTATION

17 COSATI CODES			18. SUBJECT TERMS (Continue on reverse if necessary and identify by block number)
FIELD	GROUP	SUB-GROUP	Acoustic efficiency; root mean square (rms); wall pressure fluctuations; turbulent boundary layers; artificially generated turbulent spots; zero, favorable, and adverse pressure gradients

19. ABSTRACT (Continue on reverse if necessary and identify by block number)

Wall pressure fluctuations were measured in the plane of symmetry of turbulent spots convecting in a laminar boundary layer having zero, favorable and adverse pressure gradients. The results show that the magnitude of the rms wall pressure and the spectra of the turbulent spot phase of boundary layer transition are strongly influenced by the local mean flow pressure gradient. The data also verifies that boundary layer transition in the presence of an adverse pressure gradient produces rms wall pressure fluctuations which are 1.5-2.5 times larger than those found in either a zero or favorable pressure gradient.

20 DISTRIBUTION/AVAILABILITY OF ABSTRACT			21 ABSTRACT SECURITY CLASSIFICATION	
☐ UNCLASSIFIED/UNLIMITED	☒ SAME AS RPT	☐ DTIC USERS	UNCLASSIFIED	
22a. NAME OF RESPONSIBLE INDIVIDUAL		22b. TELEPHONE (include Area Code)		22c. OFFICE SYMBOL
T.S. Mautner		(619) 225-2461		Code 634

DD FORM 1473, 84 JAN   83 APR EDITION MAY BE USED UNTIL EXHAUSTED ALL OTHER EDITIONS ARE OBSOLETE

CONTENTS

TABLES

FIGURES

i

INTRODUCTION

Knowledge of the wall pressure fluctuations beneath transitional and turbulent flows is required in order to understand and reduce aerodynamically and hydrodynamically generated noise. Measurements inside and outside turbulent boundary layers indicate that the wall pressure fluctuations generated by turbulence may well be the dominant mechanism in the generation of near field noise (self-noise) and, if the wall pressure fluctuations are coupled with the vibratory modes of the structure, there will be a significant increase in the sound level radiated into the far field.[1]

Many detailed investigations have been performed on the fluctuating wall pressure beneath turbulent boundary layers[2], utilizing both transducers mounted flush with the wall and those fitted with pinhole caps. Emmerling et al [3] and Bull and Thomas [4] have summarized the available experimental results, which show significant high frequency contributions to the pressure spectrum when the transducer size is reduced such that $dU_\tau/\nu < 100$, where d is the transducer diameter, U_τ is the friction velocity and ν is the viscosity. Their summaries are reproduced in table 1 and figure 1.

In comparison to the turbulent boundary layer results, only a limited amount of data is available on the wall pressure fluctuations associated with natural transition and, more specifically, individual turbulent spots. The measurements of DeMetz and Cassarella [5] and Huang and Hannan [6] have established certain statistical properties, in terms of intermittency, of the wall pressure fluctuations during natural transition. It is not possible to infer individual spot properties from these measurements since the spots were occuring randomly and their measurements were made at uncontrollable locations within the spots. However, DeMetz and Cassarella concluded that the magnitude of the intermittent wall pressure bursts during natural transition is approximately equal to the values measured in zero pressure gradient turbulent boundary layers. Also, the measurements of Huang and Hannan show that the rms wall pressure fluctuations during natural transition, in the presence of a strong adverse pressure gradient, were 2-3 times larger than those found in a turbulent boundary layer.

Table 1. Measurements of turbulent boundary layer wall pressure fluctuations on smooth walls in air.

Investigator	U_∞ (m/s)	$\dfrac{dU_\tau}{\nu}$	$\dfrac{(p'^2)^{1/2}}{q}$	Transducer Type	Pressure Gradient	Symbol Fig. 1
Willmarth & Roos [13]	62	198	5.4	Flush	Zero	⬦
		712	4.7			
Schloemer [9]	24	101	5.2	Flush	Zero	◇
	32	131	5.2			
	41	215	5.0	Flush	Mild Favorable	✕
	48	247	5.0			
	32	105	7.8	Flush	Mild Adverse	✚
	44	141	7.8			
Bull [15]	100	159	5.0	Flush	Zero	▽
		172	4.8			
Blake [14]	22	45	10.6	Pinhole	Zero	▲
	50	87	7.8			
Emmerling et al [3]	8.5	18	10.9	Pinhole	Zero	■
		47	9.3	Flush		□
		202	5.3			
Bull & Thomas [4]		47	6.8	Flush	Zero	○
		57	6.6			
		71	6.3			
		46	8.5	Pinhole	Zero	●
		57	8.1			
		70	7.7			
Burton [10]	24	60	10.3	Pinhole	Strong Favorable	★
	37	102	10.0			
	50	134	9.8			
	30	38	7.8-8.4*	Pinhole	Strong Adverse	✸
			8.0-10.0			
Huang & Hannan [6]	46		15.0	Pinhole	Mild Adverse	

*Normalized by local q

Figure 1. Variation of measured rms pressure fluctuations with transducer size and type ✚ current measurements; See table 1 for the additional symbols.

The purpose of this paper is to report experimental data on the rms wall pressure fluctuations associated with artificially generated turbulent spots convecting in a laminar boundary layer. The spot data, for zero, favorable and adverse (unfavorable) pressure gradients, will be compared to the available wall pressure data in order to identify the relationship between the rms wall pressure fluctuations of a spot and that measured during natural transition and in turbulent boundary layers. Since wall pressure fluctuations are a direct measure of the surface excitation forces produced by a boundary layer, flow data of this type are needed to evaluate the vibrational and hydroacoustic responses of a structure.

MEASUREMENTS

The present measurements were made at a nominal free stream velocity of $U_\infty = 10$ m/s in the closed-circuit wind tunnel of the Department of Applied Mechanics and Engineering Sciences at the University of California, San Diego. The flat plate on which the spots were generated and the other experimental apparatus were the same as that used in some previous studies [7,8]. The measured laminar boundary layer pressure gradients are indicated by the Falkner-Skan parameter, β, in table 2.

Table 2. RMS wall pressure fluctuations for turbulent spots.

Pressure Gradient	x(cm)	U_∞(m/s)	β	$(p'^2)^{1/2}/q$ Mean	$(p'^2)^{1/2}/q$ Standard Deviation
Zero	91.4	10.1	0	0.010	0.0005
	121.9	10.1	0	0.014	0.0009
	152.4	10.1	0	0.010	0.0005
Favorable	91.4	10.0	0.3	0.010	0.0005
	121.9	10.0	0.3	0.011	0.0005
	152.4	10.0	0.3	0.010	0.0005
Adverse	91.4	10.0	0.3	0.027	0.0011
	121.9	10.0	0.3	0.016	0.0004
	152.4	10.0	0.1	0.022	0.0006

The centerline turbulent spot data were obtained at longitudinal positions x=91.4, 121.9 and 152.4 cm downstream of the leading edge. The wall pressure fluctuations were measured using a B&K model 4138 0.32-cm-diameter condenser microphone whose sensing area was reduced by using a 0.8-mm-diameter pinhole in the plate's surface. The microphone was connected to a B&K 2609 measuring amplifier. For each spot the wall pressure signature was represented by 2048 digital samples, the sampling being triggered by the spot generator (x=30.4 cm) signal. For the pressure record from each spot, the rms value $(p'^2)^{1/2}$ was calculated. Then for 500 values of $(p'^2)^{1/2}$, at a particular x location and pressure gradient, the mean value, $\overline{(p'^2)^{1/2}}$, and the standard deviation were calculated.

RESULTS AND DISCUSSION

The calculated values of the turbulent spot's rms wall pressure fluctuations are summarized in table 2, and the results for the zero and favorable pressure gradients are shown in figure 1. The results show that $(p'^2)^{1/2}/q$ (q is the free stream dynamic pressure) for the zero and favorable pressure gradients are approximately equal to the values measured by "pinhole" transducers in zero pressure gradient turbulent boundary layers (table 1 and figure 1). The one exception, in the current results, is the zero pressure gradient data at x=121.9 cm, where the higher value of $(p'^2)^{1/2}$ is attributed to a slight variation in the pressure gradient along the flat plate. The equal magnitude of the spot's $(p'^2)^{1/2}$ for both the zero and favorable pressure gradient is in qualitative agreement with, for example, the results of Schloemer [9] and Burton [10].

However, when subjected to an adverse pressure gradient, the turbulent spot's rms wall pressure fluctuations are 1.7 - 2.7 times larger than either the zero or favorable pressure gradient results (table 2). The measured increases are in general agreement with the results of Huang and Hannan [6]. They found $(p'^2)^{1/2}/q \simeq 0.038$ during natural transition on a forebody of revolution subjected to a strong adverse pressure gradient as compared to $(p'^2)^{1/2}/q \simeq 0.015$ in a turbulent boundary layer with a mild, adverse pressure gradient. The increased $(p'^2)^{1/2}$ for the turbulent spot, and presumably for natural transition, is consistent with the larger velocity fluctuations (u') [8] found in the adverse pressure gradient flow as compared to u' for a spot in a zero pressure gradient flow [11]. Higher velocity fluctuations were also measured by Schloemer [9] and Burton [10] in their adverse pressure gradient turbulent boundary layers. The 40% reduction in the spot's $(p'^2)^{1/2}$ from x=91.4 to 121.9 cm is due to the spot's adjustment to the constant pressure gradient region. This adjustment plus the subsequent 30% increase in $(p'^2)^{1/2}$ from x=121.9 to 152.4 cm indicate the sensitivity of the spot's $(p'^2)^{1/2}$ magnitude to the local mean flow pressure gradient.

For a boundary layer, Kraichnan [12] formulated a qualitative relationship between the pressure and shear forces which states that the ratio of the rms wall pressure and the wall shear stress (τ_w) equals a constant, $(\overline{p'^2})^{1/2}/\tau_w = C = 6$. Recent, experimental results have determined that the constant C is on the order of 3 with typical values of 2.6 found by Willmarth and Roos [13] and 3.4 by Blake [14]. For the current zero and favorable pressure gradient spot data, the ratio of the $(\overline{p'^2})^{1/2}$ values in table 2 and τ_w calculated using Prandtl's equation

$$(U_\tau/U_\infty)^2 = 0.0296 \, R_{ex}^{-1/5}, \quad R_{ex} = xU_\infty/\nu, \quad U_\tau = (\tau_w/\rho)^{1/2}$$

yield a range of values for C of 2.5-3.5. This calculation shows that both the zero and favorable pressure gradient spot data scale well with the wall
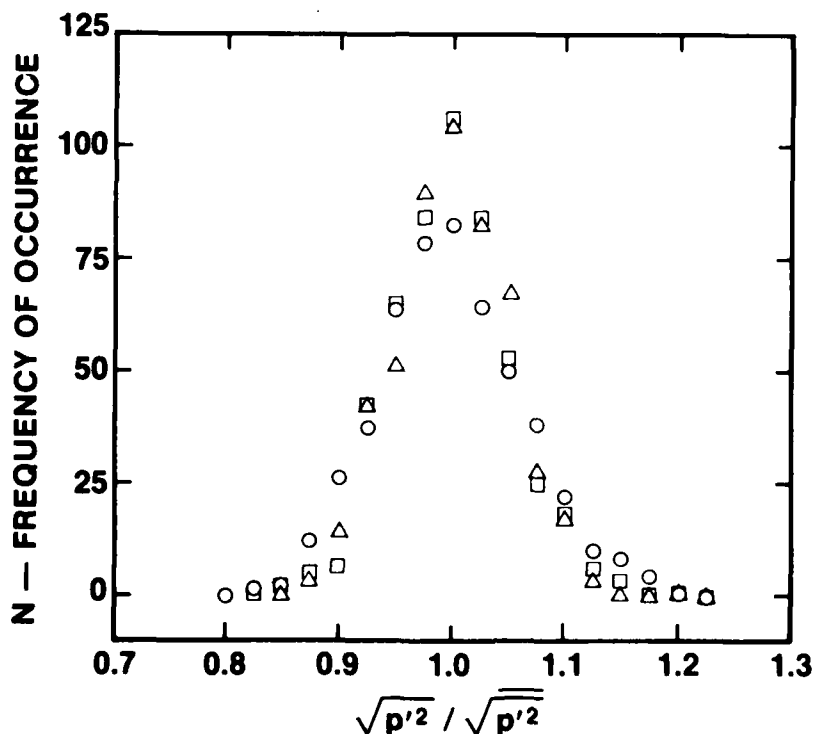
Figure 2. Frequency of occurrence distribution of the RMS pressure for 500 spots — zero pressure gradient U_∞ = 10 m/s; $\square$, x = 91.4 cm; $\bigcirc$, x = 121.9 cm; $\triangle$, x = 152.4 cm.

shear stress and that the results are consistent with the zero pressure gradient turbulent boundary layer results. However, when the unfavorable pressure gradient spot $(p'^2)^{1/2}$ data are normalized by τ_w, a value of C=12 is obtained. In order to obtain $C \simeq 3$, an unrealistic value of $U_\tau/U_\infty \simeq 0.064$ would be required, indicating that the adverse pressure gradient spot results do not scale with the local wall shear stress. A similar result was found by Burton [10] for a turbulent boundary layer with an adverse pressure gradient.

Thus far the measurements of the wall pressure fluctuations asociated with translational and turbulent flows have been characterized by a single value of $(p'^2)^{1/2}$, which is representative of a mean flow condition. This method is satisfactory in characterizing the statistically steady properties of a turbulent boundary layer. However, the final stage of boundary layer transition is composed of randomly occurring spots, and previous measurements of $(p'^2)^{1/2}$ during natural transition have not identified the statistical distribution of the spot's $(p'^2)^{1/2}$ magnitude nor its relationship to the generation of acoustic noise.

To examine the variation of $(p'^2)^{1/2}$ about its mean value, plots of the frequency of occurrence N of a particular magnitude $(p'^2)^{1/2}$ as a function of $(p'^2)^{1/2}/\overline{(p'^2)^{1/2}}$ were constructed. For each pressure gradient, the values of $(p'^2)^{1/2}$ from 500 spots at each x location were categorized using 0.5 standard deviation bandwidth. The results in figures 2-4 show that, for each pressure gradient, the N distributions at each x exhibit excellent similarity. The N distributions for the zero and favorable pressure gradients (figures 2-3) are approximately equal and the $(p'^2)^{1/2}$ magnitudes are broadly distributed about the mean. In contrast, N distributions for the adverse pressure gradient (figure 4) show a 20-25% increase in the number of $(p'^2)^{1/2}$ values occurring at the mean and that the remaining $(p'^2)^{1/2}$ values are more concentrated about the mean. This character of the N distribution indicates that, even though $(p'^2)^{1/2}$ is a broadband property of the wall pressure field, the small variation in the magnitude of $(p'^2)^{1/2}$ in the adverse pressure gradient data would provide a stronger driving force on a structure which may result in higher self- and radiated noise levels.

7
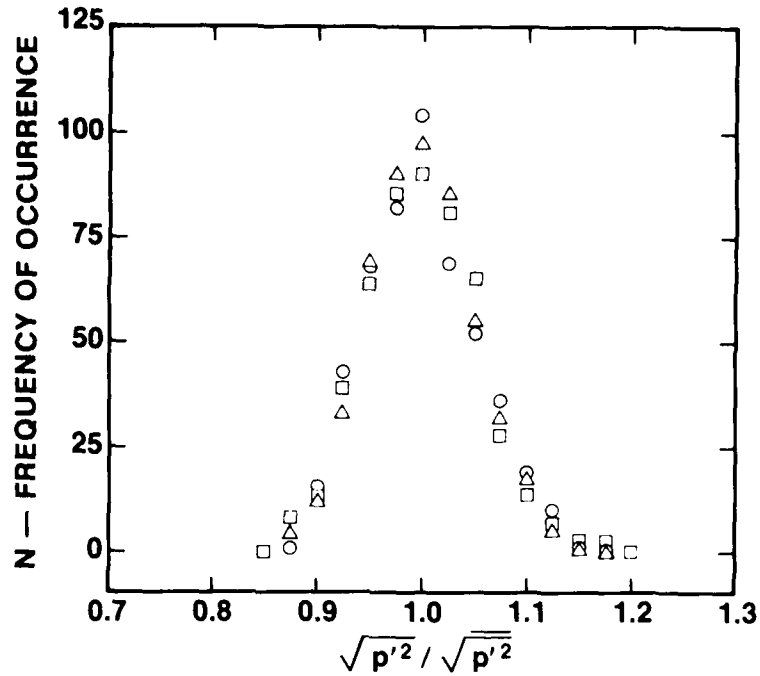
Figure 3. Frequency of occurrence distribution of the rms pressure for
500 spots — favorable pressure gradient U $_\infty$ = 10 m/s; □, x = 91.4 cm;
O , x = 121.9 cm; △ , x = 152.4 cm.
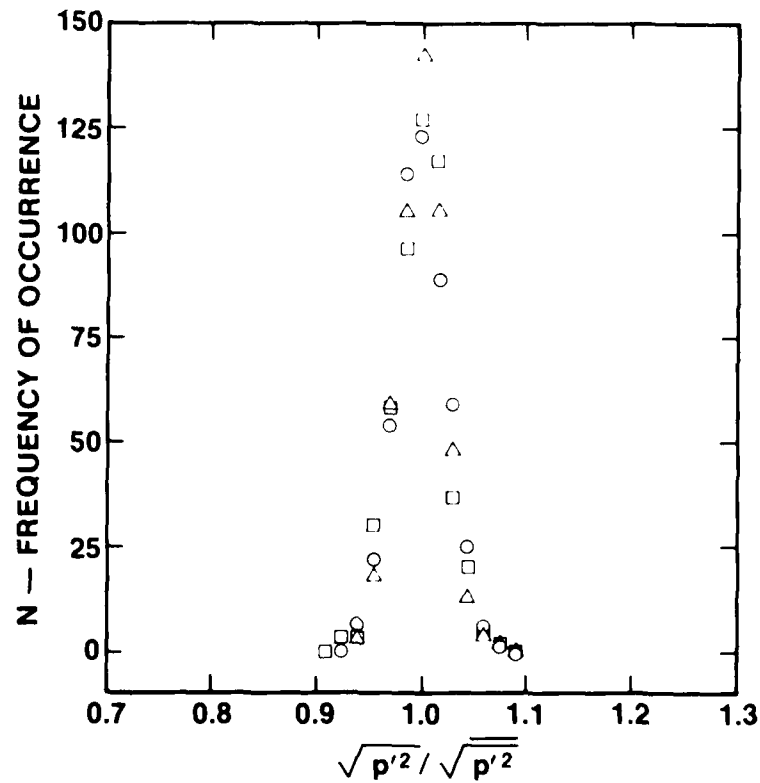
Figure 4. Frequency of occurrence distribution of the rms pressure for
500 spots — adverse pressure gradient U$_\infty$ = 10 m/s; □, x = 91.4 cm;
O , x = 121.9 cm; △, x = 152.4 cm.

8

The N distributions provide information about the variation of $(p'^2)^{1/2}$ over a large number of spots; however, they do not provide any information about the contribution of the spot's "random" wall pressure fluctuations in determining the value of $(p'^2)^{1/2}$. To examine this issue, probability density functions were calculated. For each pressure gradient at x=152.4 cm, the probability density function for 500 spots were calculated and then averaged. The calculated probability density functions, B(p'), shown in figure 5 are given in terms of B(p')Δp', which represents the fraction of the total p' samples in the p' to p'+Δp' band (p'/Δp'=0 occurs at $(\overline{p'^2})^{1/2}$). The results show that B(p') for all three pressure gradients are nearly equal and that small positive values of p' are more probable than small negative values of p'. It is this statistical nature of p' that not only results in the 1.5 - 2.5 increase in $(p'^2)^{1/2}$, but also, like the N distributions, indicates the presence of an intense wall pressure field during boundary layer transition under the influence of an adverse pressure gradient.

The calculated values of $(p'^2)^{1/2}$ and the N distributions provide broadband (in frequency) information about the turbulent spot. To obtain the distribution of energy with frequency, the spectra of the spot's wall pressure field were computed from the finite length, digitized time series p(t). For each pressure gradient at x=152.4 cm, the spectra, Φ(f), from 100 spots were calculated and then averaged. The nondimensional spectra are presented in figure 6, where f is the frequency and δ* is the boundary layer displacement thickness. No corrections for the finite size of the transducer were applied to the spectra.

The spot's zero and favorable pressure gradient spectra (figure 6 a and b) are approximately equal and verify the nearly equal magnitudes of $(p'^2)^{1/2}$ given in table 2. These spectra are also in qualititative agreement with the turbulent boundary layer results of Blake [14], Bull [15] and Burton [10] for a zero pressure gradient and Schloemer [9] for a mild, adverse pressure gradient. The lower values of Schloemer's zero and favorable pressure gradient spectra are probably due to his larger transducer size and lower turbulent intensities.
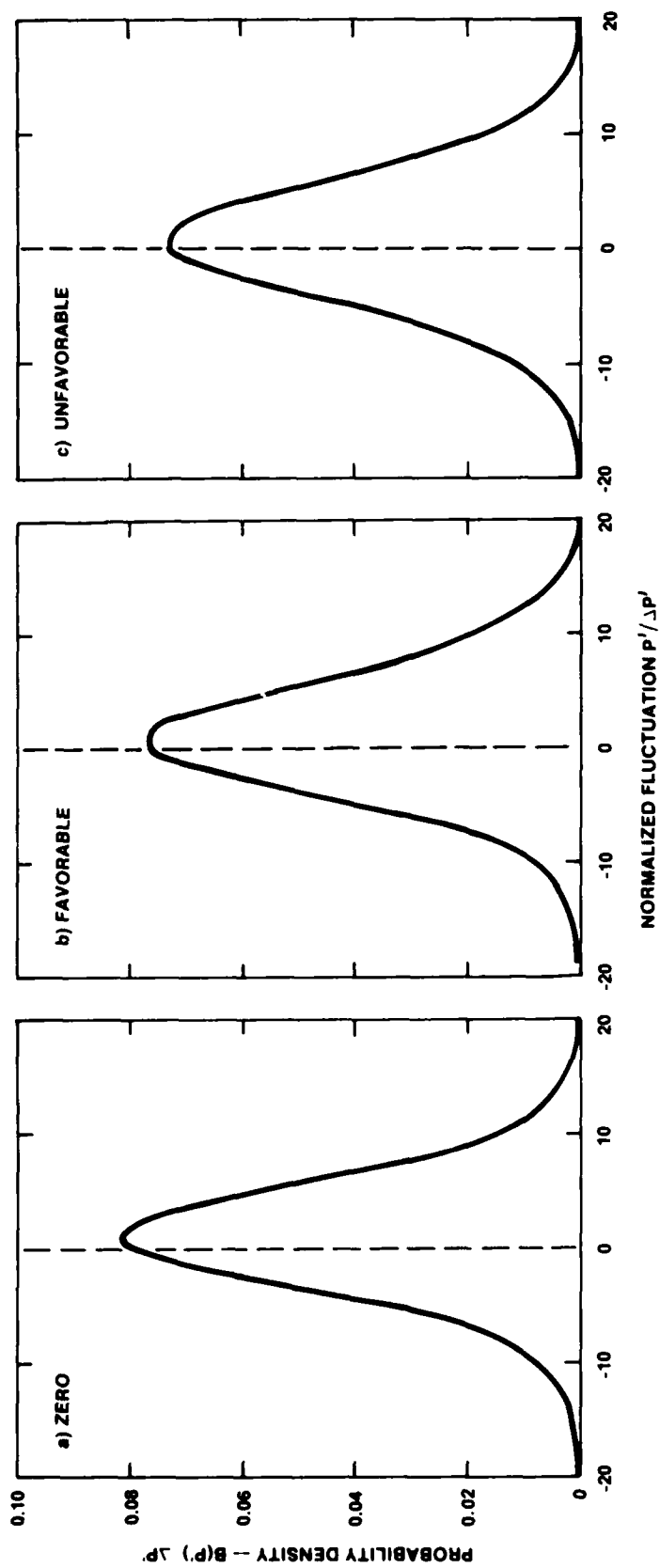
Figure 5. Probability density function of p'. $U_\infty = 10$ m/s; $x = 152.4$ cm: a) zero; b) favorable; and c) unfavorable (adverse) pressure gradients.
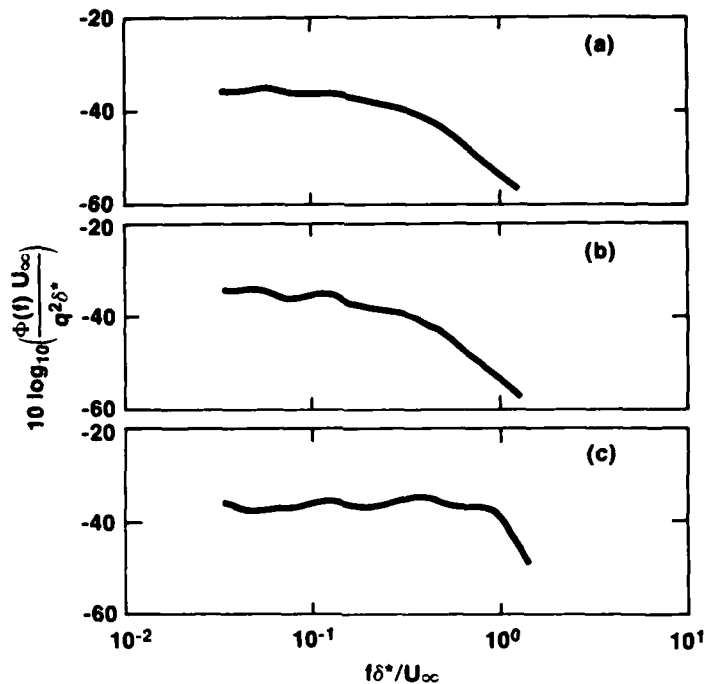
Figure 6. Comparison of the nondimensional power spectrum for a) zero,
b) favorable and c) adverse pressure gradients.

For the adverse pressure gradient, the spot's wall pressure spectrum shows a nearly constant magnitude with frequency, which is in contrast to the rapid spectral decrease with increasing frequency found for both zero and favorable pressure gradient spectra. Schloemer pointed out that the adverse pressure gradient spectrum for a turbulent boundary layer has a larger magnitude, especially at lower frequencies, due to the increase in the longitudinal turbulent intensities (u') near the wall, $y/\delta_t < 0.6$ (δ_t - turbulent boundary layer thickness). Similarily, the distribution of u' with y in current spot data [8] shows a higher level of u' throughout the central region as compared to the zero pressure gradient spot data of Antonia et al[11], thereby producing the increased magnitude of both the spectrum and $(p'^2)^{1/2}$.

Lauchle [16] has derived an expression for the acoustic efficiency of boundary layer transition and compared it to the acoustic efficiency of a turbulent boundary layer. He determined that the flow noise generated by boundary layer transition is more efficiently radiated into the far field than the

11

noise generated by a fully developed turbulent boundary layer (approximately 3 orders of magnitude in his example). At least for the current adverse pressure gradient spot data, the nearly constant magnitude of the spectra would indicate a greater possibility of the spot's wall pressure field coupling with both the structure and the propagating modes of the acoustic field to produce more intense near and far field noise levels.

CONCLUSIONS

The current experimental results show that the magnitude of $(p'^2)^{1/2}$ and the spectra of the turbulent spot phase of boundary layer transition are strongly influenced by the local mean flow pressure gradient. The current spot data verifies the results of Huang and Hannan [6] and shows that boundary layer transition in the presence of an adverse pressure gradient will result in $(p'^2)^{1/2}$ values which are approximately 1.5 - 2.5 times larger than that found for a zero or favorable pressure gradient. Additionally, the nearly constant magnitude of the spot's adverse pressure gradient spectrum indicates a nearly even distribution of energy with frequency.

The above results indicate that a transitional flow, when subjected to an adverse pressure gradient, will produce a stronger driving force on a structure over a wide frequency range. This condition may lead to a higher degree of coupling between the wall pressure field and the structure resulting in higher levels of both structure borne (self-noise) and fluid borne (far field) noise levels.

REFERENCES

1. J. Ffowes Williams. 1969. Hydrodynamic noise. <u>Annual Review of Fluid Mechanics 1</u>, 1:197-222.

2. W. Willmarth. 1975. Pressure fluctuations beneath turbulent boundary layers. <u>Annual Review of Fluid Mechanics</u>, 7:13-38.

3. R. Emmerling, G. Meier and A. Dinkelacker. 1973. Investigation of the instantaneous structure of the wall pressure under a turbulent boundary layer. <u>AGARD Conference Proceedings Number 131 on Noise Mechanisms</u>, 24.1-24.11.

4. M. Bull and A. Thomas. 1976. High frequency wall pressure fluctuations in turbulent boundary layers. <u>Physics of Fluids</u>, 19:597-598.

5. F. DeMetz and M. Casarelia. 1973. An experimental study of the intermittent properties of the boundary layer pressure field during transition on a flat plate. <u>NSRDC Report No. 4140</u>.

6. T. Huang and D. Hannan. 1975. Pressure fluctuations in the region of flow transition. <u>DTNSRDC Report No. 4723</u>.

7. T. Mautner and C. Van Atta. 1982. An experimental study of the wall pressure field associated with a turbulent spot in a laminar boundary layer. <u>Journal of Fluid Mechanics</u>, 118:59-77.

8. T. Mautner. 1983. <u>Investigation of the Wall Pressure, Wall Shear Stress and Velocity Fields Associa ed with a Turbulent Spot in a Laminar Boundary Layer</u>. Ph.D. Thesis, University of California, San Diego.

9. H. Schloemer. 1967. Effects of pressure gradients on turbulent boundary layer wall pressure fluctuations. <u>Journal of the Acoustical Society of America</u>, 42:93-113.

10. T. Burton. 1973. Wall pressure fluctuations at smooth and rough surfaces under turbulent boundary layers with favorable and adverse pressure gradients. <u>M.I.T. Acoustics and Vibration Laboratory Report No. 70208-9</u>.

11. R. Antonia, A. Chambers and C. Van Atta. 1981. Simultaneous temperature and velocity measurements in the plane of symmetry of a transitional turbulent spot. <u>Journal of Fluid Mechanics</u>, 108:317-343.

12. R. Kraichnan. 1956. Pressure fluctuations in turbulent flow over a flat plate. <u>Journal of Acoustical Society of America</u>, 28:378-390.

13. W. Willmarth and F. Roos. 1965. Resolution and structure of the wall pressure field beneath a turbulent boundary layer. <u>Journal of Fluid Mechanics</u>, 22:81-94.

14. W. Blake. 1970. Turbulent boundary layer wall pressure fluctuations on smooth and rough walls. <u>Journal of Fluid Mechanics</u>, 44:637-660.

15. M. Bull. 1967. Wall pressure fluctuations associated with subsonic turbulent boundary layer flow. <u>Journal of Fluid Mechanics</u>, 28:719-754.

16. G. Lauchle. 1978. Acoustic efficiency of boundary layer transition. <u>ARL/PSU TM78-285</u>.

END

FILMED

1-86

DTIC